RESEARCH ARTICLE

Role of autonomic, nociceptive, and limbic brainstem nuclei in core autism features

Brittany G. Travers[1,2] | Olivia Surgent[1] | Jose Guerrero-Gonzalez[1,3] |

Douglas C. Dean III[1,3,4] | Nagesh Adluru[1,5] | Steven R. Kecskemeti[1] |

Gregory R. Kirk[1] | Andrew L. Alexander[1,3,6] | Jun Zhu[7] | Emily C. Skaletski[1,2] |

Sonali Naik[1] | Monica Duran[1]

[1]Waisman Center, University of Wisconsin-Madison, Madison, Wisconsin, USA

[2]Department of Kinesiology, Occupational Therapy Program, University of Wisconsin-Madison, Madison, Wisconsin, USA

[3]Department of Medical Physics, University of Wisconsin-Madison, Madison, Wisconsin, USA

[4]Department of Pediatrics, University of Wisconsin-Madison, Madison, Wisconsin, USA

[5]Department of Radiology, University of Wisconsin-Madison, Madison, Wisconsin, USA

[6]Department of Psychiatry, University of Wisconsin-Madison, Madison, Wisconsin, USA

[7]Department of Statistics, University of Wisconsin-Madison, Madison, Wisconsin, USA

Correspondence
Brittany G. Travers, Waisman Center, University of Wisconsin-Madison, 1500 Highland Avenue, Room 435, Madison, WI 53705, USA.
Email: btravers@wisc.edu

Abstract

Although multiple theories have speculated about the brainstem reticular formation's involvement in autistic behaviors, the in vivo imaging of brainstem nuclei needed to test these theories has proven technologically challenging. Using methods to improve brainstem imaging in children, this study set out to elucidate the role of the autonomic, nociceptive, and limbic brainstem nuclei in the autism features of 145 children (74 autistic children, 6.0–10.9 years). Participants completed an assessment of core autism features and diffusion- and T1-weighted imaging optimized to improve brainstem images. After data reduction via principal component analysis, correlational analyses examined associations among autism features and the microstructural properties of brainstem clusters. Independent replication was performed in 43 adolescents (24 autistic, 13.0–17.9 years). We found specific nuclei, most robustly the parvicellular reticular formation-alpha (PCRtA) and to a lesser degree the lateral parabrachial nucleus (LPB) and ventral tegmental parabrachial pigmented complex (VTA-PBP), to be associated with autism features. The PCRtA and some of the LPB associations were independently found in the replication sample, but the VTA-PBP associations were not. Consistent with theoretical perspectives, the findings suggest that individual differences in pontine reticular formation nuclei contribute to the prominence of autistic features. Specifically, the PCRtA, a nucleus involved in mastication, digestion, and cardio-respiration in animal models, was associated with social communication in children, while the LPB, a pain-network nucleus, was associated with repetitive behaviors. These findings highlight the contributions of key autonomic brainstem nuclei to the expression of core autism features.

Lay Summary

Looking at brain scans of 145 autistic and non-autistic children and testing our results again in 45 autistic and non-autistic adolescents, we found that a particular part of the brainstem thought to be involved in chewing, digesting food, heart rate, and breathing was related to social communication. Another part of the brainstem thought to be involved in processing painful sensations was associated with preferring things not to change and preferring to stick with certain routines.

This information further supports the involvement of the brainstem in the expression of autism features.

INTRODUCTION

Social communication challenges and restricted and repetitive behaviors are core diagnostic criteria for autism spectrum disorder (American Psychiatric Association, 2013), but the brain basis of these multifaceted behaviors is still being revealed. Social cognition is thought to be subserved by a broad network of brain structures, including the prefrontal, somatosensory, and temporal cortices, as well as the subcortical amygdala, hypothalamus, and basal ganglia (for a review, see Fernández et al., 2018). In parallel, restricted and repetitive behaviors span a diversity of behaviors that can be broken down into the domains of circumscribed interests, insistence on sameness, and stereotyped movements (Lam et al., 2008; Supekar et al., 2021). Restricted and repetitive behaviors are thought to be subserved by the cortico-basal-ganglia-thalamo-cortical network (Casado-Sainz et al., 2022; Lefebvre et al., 2023; Schuetze et al., 2016; Weeland et al., 2022), with different domains of repetitive behaviors being related to different time-varying cross-network interactions (Supekar et al., 2021). Despite what we are learning about the brain basis of these behaviors, the brainstem is conspicuously missing from these networks, even though the brainstem has connections to all the aforementioned brain regions (Cauzzo et al., 2022; Legg et al., 1989; Singh et al., 2022; Tervo et al., 2016). This is a critical omission as 60 years ago, the first biology-based theories of autism (Hutt et al., 1964; Rimland, 1964) postulated that the brainstem's reticular formation was consistent with the cognitive and behavioral features observed in autistic individuals. More recent reviews of behavioral, animal, postmortem, and imaging literatures further suggest that brainstem functions are consistent with behavioral features in autism (Burstein & Geva, 2021; Dadalko & Travers, 2018; Delafield-Butt & Trevarthen, 2018; Trevarthen & Delafield-Butt, 2013), and the increasingly popular polyvagal theory of autism (Porges, 2003, 2005) suggests that specific nuclei of the brainstem are implicated in social differences in autism. However, the brainstem's role in autism has remained mostly theoretical, as investigations that focus on the brainstem in living, autistic humans have been limited to gross brainstem measures, such as the brainstem's overall size (Bosco et al., 2019; Jou et al., 2009), shape (Bosco et al., 2019), or primary descending pathways (Travers et al., 2015). Therefore, the brainstem remains largely an area of mystery, despite the many decades of theories suggesting its

relation to neurodevelopmental features in autistic populations.

The intricate anatomy of the brainstem has been under-explored in the human neuroimaging literature, likely due to the technical challenges of imaging the brainstem in vivo with magnetic resonance imaging (MRI) (Irfanoglu et al., 2012, 2015). Indeed, most MRI protocols and processing pipelines have been designed to image the cerebrum, not accounting for the brainstem's small size and unique anatomical intertwining of white matter tracts surrounding gray matter nuclei. As such, it is possible that even studies that have included the brainstem in whole-brain analyses may not have had the resolution or coverage to accurately detect group or individual differences in this area (Guerrero-Gonzalez et al., 2022). Recently, our lab implemented acquisition and post-processing methods to enhance brainstem imaging in autistic children (Guerrero-Gonzalez et al., 2022). In applying these techniques, we found that brainstem white matter tracts were related to individual differences in sensory features, primarily hyporesponsiveness, and tactile responsivity, in autistic children (Surgent et al., 2022). While these findings suggest that brainstem white matter may be implicated in sensory features commonly reported in autism, still no study has tested the early biology-based theories of autism (Hutt et al., 1964; Rimland, 1964) by looking at specific gray matter nuclei of the reticular formation in reference to the behavioral features that are requisite for an autism diagnosis (American Psychiatric Association, 2013). As such, this study set out to investigate the microstructural properties of brainstem nuclei in reference to individual differences in core autism diagnostic features.

Brainstem nuclei are known to have overlapping involvement in sensory, motor, arousal/consciousness, and autonomic/nociceptive/limbic functions (see Singh et al., 2022). For the current investigation, we focused on autonomic, nociceptive, and limbic brainstem nuclei that are central to homeostatic functions (i.e., cardio-respiration, gut function, thermoregulation, etc.), reflexive emotional responses (for a review see Venkatraman et al., 2017), and response to pain or threats (for a review see Martins & Tavares, 2017). This focus was based on theories such as the polyvagal theory of autism (Porges, 2003, 2005) and the neurovisceral integration theory (Thayer & Lane, 2000) which suggest that atypical autonomic arousal may lead to social and emotional differences in autistic individuals. While these theories offer considerable explanatory promise, reviews of this

literature (Arora et al., 2021; Benevides & Lane, 2015; Cuve et al., 2018; Lydon et al., 2016; Moore, 2015) highlight that individual differences may be present in pain and autonomic functioning, but group differences are not consistently found. It is possible that understanding the brainstem nuclei that participate in whole-brain pain, emotional, and cardiorespiratory networks may help explain the high degree of individual variability among autistic individuals.

Brainstem nuclei involved in autonomic/nociceptive/limbic functions can be found from the medulla to the midbrain. These nuclei include multiple aspects of the reticular formation (parvicellular reticular nucleus-alpha part [PCRtA], superior and inferior medullary reticular formation [iMRT; sMRt], medial and lateral parabrachial nuclei [MPB; LPB], raphe nuclei [dorsal raphe {DR}, raphe magnus {Rm}, pallidus {Rp}, and obscurus {RoB}], locus coeruleus [LC]), as well as the ventral-tegmental area parabrachial pigmented nucleus complex (VTA-PBP), viscerosensory motor nuclei (VSM) and the periaqueductal gray matter (PAG). While these autonomic/pain/limbic brainstem structures have been most extensively studied in animal models, recent high-resolution imaging has demonstrated general conservation of the structural connectivity (Singh et al., 2022) and functional connectivity (Cauzzo et al., 2022) of brainstem regions in human beings.

Therefore, the aim of the present study was to use a brainstem-optimized image acquisition and post-processing methods (Guerrero-Gonzalez et al., 2022) combined with a mapping of the autonomic/pain/emotion brainstem nuclei (Bianciardi et al., 2015, 2018; García-Gomar et al., 2019, 2022; Singh et al., 2019, 2021) to test if microstructural properties of brainstem relate to individual variation in core social and repetitive-behavior features in autistic children. Children with no known diagnosis of autism or other neurodevelopmental conditions (i.e., "non-autistic" children) are included for context and for examining these associations across the broader population, but they are not included for direct group comparisons, as the autonomic literature suggests greater within-group than between-group variation. Because of the need for increasing sample sizes and/or replication in imaging studies (Marek et al., 2022), two distinct data sets from our lab were used to achieve these aims.

Given the theoretical evidence on the brainstem's role in autism-related behaviors, we hypothesized that individual differences in the microstructure of specific groupings of the autonomic/emotion/pain brainstem nuclei would relate to individual variation in the prominence of social and repetitive-behavior features. Understanding the pattern of brainstem involvement in social communication and repetitive behavior features has the potential to unveil a more complete depiction of whole-brain involvement in autism, as the brainstem nuclei are key connection points for brain-wide circuits involved in

autonomic, limbic, and pain functions (Cauzzo et al., 2022; Singh et al., 2022).

METHODS

Participants

The study conformed to the standards of the US Federal Policy for the Protection of Human Subjects. The Institutional Review Board at the University of Wisconsin-Madison prospectively reviewed and approved all procedures (IRB #2018-1067). All children provided assent and all parents and/or guardians provided informed consent.

This cross-sectional study included a final sample of 74 autistic children (6.14–10.99 years old, 15 female) and 71 non-autistic children (age range 6.02–10.80 years, 24 female). Groups were matched on chronological age to control for age-related biological changes that occur in brainstem structures. Table 1 contains group-level demographic information. All participants were required to communicate using spoken language. None of the participants had a previous diagnosis of tuberous sclerosis, Down syndrome, fragile X, hypoxia-ischemia, notable and uncorrected hearing or vision loss, or a history of severe head injury.

Autistic participants were required to enter the study with a previous diagnosis of autism spectrum disorder. Additionally, autistic participants were required to meet cutoff on the Autism Diagnostic Observation Schedule, 2nd edition (ADOS-2) (Lord et al., 2012) or the Autism Diagnostic Interview-Revised (ADI-R) (Rutter, Le Couteur, & Lord, 2003). However, six participants barely missed cutoff on the ADOS-2, but they were included after a record review with a licensed clinical psychologist. All six met cutoff on both the Social Responsiveness Scale, Second Edition (SRS-2) (Constantino & Gruber, 2012) and the Social Communication Questionnaire (SCQ) (Rutter, Bailey, & Lord, 2003). See Supporting Information for additional information regarding diagnostic group criteria and specifics of the diagnostic methods before and during the COVID-19 pandemic.

T A B L E 1   Demographic information of participants.

Characteristic	Autistic ($n = 74$)	Non-autistic ($n = 71$)
Sex (male %)	59/74 (80%)	47/71 (66%)
Age (years)	8.56 (6.14–10.99)	8.22 (6.02–10.80)
Full scale IQ	105.44 (66–147)	115.07 (88–145)
Average head motion (AVD)	0.66 (0.18–2.04)	0.56 (0.16–2.99)
Taking centrally active medication	29/74 (39%)	0/71 (0%)

Behavioral measures of autism features

Autism features were measured using caregiver reports of the SRS-2 (Constantino & Gruber, 2012), the SCQ (Rutter, Bailey, & Lord, 2003), and the Repetitive Behavior Scale-Revised (RBS-R) (Bodfish et al., 1999). The principal component summary of autism features included SRS-2, SCQ, and RBS-R total raw scores. Raw scores were used because the SCQ and RBS-R do not have age-normed standard scores and the SRS-2 standard scores do not vary within this sample's age range. Follow-up analyses examined the SRS-2 domain scores of social awareness, social cognition, social communication, social motivation, and restricted/repetitive behaviors, and the RBS-R domain scores of stereotyped, self-injurious, compulsive, ritualistic, sameness, and restricted behaviors. RBS-R total and domain scores were log-transformed in all analyses to meet the assumptions of normality.

Imaging acquisition and processing

MRI data were acquired on a 3T GE Discovery MR750 scanner (Waukesha, WI) with a 32-channel phased array head coil (Nova Medical, Wilmington, MA). A multi-shell spin-echo echo-planar imaging (EPI) pulse sequence was used to acquire diffusion weighted images (DWIs) (9 directions at $b = 350$ s/mm^2, 18 directions at $b = 800$ s/mm^2, and 36 directions at $b = 2000$ s/mm^2, and 6 non-diffusion-weighted [$b = 0$ s/mm^2] volumes; TR/TE = 9000/74.4 ms; FOV = 230 mm × 230 mm, in-plane resolution 2.4 mm × 2.4 mm, interpolated to 1.8 mm × 1.8 mm; 76 slices, slice thickness 3.6 mm, slice spacing 1.8 mm). Six additional reverse phase-encoded non-diffusion-weighted volumes were collected to correct for susceptibility-induced artifacts (Andersson et al., 2003). Whole-brain structural images were collected using a 3D T1-weighted MPnRAGE sequence with 1-mm isotropic resolution (Kecskemeti et al., 2016, 2018). Even with considerable head motion, retrospective head-motion correction with MPnRAGE has been shown to allow for highly repeatable tissue-specific segmentation and quantitative T1 mapping (Kecskemeti et al., 2021; Kecskemeti & Alexander, 2020a, 2020b).

DWIs were processed to reduce noise (Veraart et al., 2016), Gibbs ringing (Kellner et al., 2016), and artifacts caused by motion, eddy currents (Andersson et al., 2016, 2017; Andersson & Sotiropoulos, 2016; Bastiani et al., 2019), and EPI distortions (Andersson et al., 2003). To enhance the apparent spatial resolution and sharpen brainstem tissue contrast, DWI data were then processed with the TiDi-Fused workflow previously described (Guerrero-Gonzalez et al., 2022; Surgent et al., 2022, 2023). Briefly, the TiDi-Fused workflow leveraged rigid-body boundary-based registration (BBR) (Greve & Fischl, 2009) to map the mean DWI $b = 0$

volume the MPnRAGE-derived T1-weighted image. This transformation was then applied to the entire DWI series with cubic b-spline interpolation (Avants, Tustison, Wu, et al., 2011) and the rotational component of the rigid body transformation was applied to the DWI encoding directions, resulting in DWIs with an apparent isotropic resolution of 1-mm.

For quality control processes and to account for head motion in analyses, the average relative voxel displacement between volumes acquired during the DWI scan was estimated (Andersson & Sotiropoulos, 2016).

DWIs were then used to estimate free water elimination diffusion tensor imaging (FWE-DTI) and neurite orientation dispersion and density imaging (NODDI) models to generate parameter maps. FWE-DTI reduces partial volume artifacts caused by cerebrospinal fluid (Hoy et al., 2014), which may especially impact brainstem estimations. Therefore, the FWE-DTI model (Fick et al., 2019) was used to fit diffusion tensors at each voxel and estimate fractional anisotropy (FWE-FA), mean diffusivity (FWE-MD), axial diffusivity (FWE-AD), and radial diffusivity (FWE-RD). NODDI, a biophysical multi-compartment model that quantifies neurite characteristics (Zhang et al., 2012), was used to generate estimates of orientation dispersion index (ODI) and intracellular volume fraction (ICVF). While NODDI is often utilized to describe white matter characteristics, it is also able to capture the highly complex neurite characteristics of gray matter microstructure (DiPiero et al., 2023; Zhang et al., 2012).

Additionally, quantitative T1 (qT1) maps were used to generate R1 estimations (R1 = 1/qT1) at each voxel using MPnRAGE images (Kecskemeti et al., 2021). While R1 can be influenced by several biological factors, it is often associated with the presence of myelination (Dick et al., 2012; Stüber et al., 2014). All FWE-DTI, NODDI, and R1 maps passed a visual inspection for processing artifacts prior to statistical analyses.

Brainstem nuclei delineation

The Brainstem Navigator atlas (Bianciardi et al., 2015, 2018; García-Gomar et al., 2019, 2022; Singh et al., 2019, 2021) was used to delineate 22 brainstem nuclei involved in autonomic, pain, and limbic function (Singh et al., 2022). Specifically, affine and diffeomorphic transformations (Avants, Tustison, Wu, et al., 2011) were used to warp the probabilistically defined brainstem regions of interest to a T1-weighted study specific template that was aligned with the MNI152 T1-weighted image. The T1-weighted study specific template was generated using MPnRAGE data using the ANTs template construction utility (buildtemplateparallel.sh) (Avants, Tustison, Song, et al., 2011). The brainstem regions of interest were then mapped to each participant's native space by applying the inverse transformations estimated during the template

formation. The brainstem regions of interest were inspected visually to ensure a faithful representation of the spatial pattern and anatomical placement in each participant's native space. Weighted median (Cormen & Cormen, 2001; Edgeworth, 1887, 1888) values of the FWE-DTI, NODDI, and R1 measures were extracted from these 22 bilateral brainstem nuclei, using the weights provided by the probabilistic atlas.

Statistical analysis

Our statistical approach was carried out according to the pre-planned analyses in our NIH grant (R01 HD094715) using R version 4.3.1 (R Core Team, 2023). Given the large number of autonomic brainstem nuclei and microstructural values of interest, a principal component analysis (PCA) using promax (an oblique rotation to allow for the factors to be non-orthogonal) was performed with the psych package (Revelle, 2023) on z-scores of the 154 variables (22 brainstem nuclei each with seven microstructural measures). Prior to running the PCA, a 13-factor structure was determined using parallel analysis from the psych package (Revelle, 2023), scree plot, Bayesian information criterion (BIC), and eigenvalues. From the PCA output, loadings shown in Table S1 were the standardized rotational loadings (factor pattern matrix) based on the correlation matrix. No thresholding of the standardized rotation loadings was performed. Instead, a continuous factor score for each participant for each of the 13 brainstem factors was generated by the PCA. These mean-centered factor scores were calculated as part of the PCA using regression. While no thresholding was performed, naming the factors was performed by highlighting variables with rotational loadings greater than |0.4|. As can be seen from Figures S1–S13 and Table S1, most of the clusters represented the bilateral nuclei of interest as well as similar measurement properties (i.e., R1 values clustered together), in support of the biological plausibility of these clusters.

Similarly, pre-planned data reduction via PCA (using non-oblique varimax) was performed with the caregiver-reported behavioral measures (total scores of the SRS-2, SCQ, and log-transformed RBS-R [for normality]), which were found to collapse onto a single factor (per parallel analysis, scree plot of eigenvalues, BIC, and root mean squared error of approximation [RMSEA]). The measures demonstrated similar sums of squares loadings onto the principal component: SRS-2 = 0.97; SCQ = 0.95; RBS-R = 0.96.

We examined potential sex differences in the brainstem and behavioral summary measures before performing analyses across the collapsed sample. There were no significant sex differences in any of the brainstem clusters, but there were significant sex differences in the summary measure of autism features, with females having decreased autism features compared to males, $t(146) = 2.69$, $p = 0.008$. Similarly, head motion and age showed trending, but non-significant relations with the autism summary measure (in addition to well-established relationships with the brainstem imaging measures). Therefore, we controlled for linear effects of age, sex, and head motion (via residualization) not only in our brainstem cluster measures but also in our behavioral measures.

Analyses centered on brainstem-behavior correlations within the group of autistic participants. However, because areas of the brainstem have not been examined in this age range previously, multiple regression analyses with the non-autistic group (main effects for autism features and diagnostic group status, while also examining potential interaction effects) were performed to contextualize the brainstem findings of the autistic group. To adjust for multiple comparisons, false discovery rate (FDR) correction (Benjamini & Hochberg, 1995) was used.

Follow-up analyses

Follow-up analyses were performed to elucidate how specific autism features may relate to the brainstem nuclei clusters identified in our primary analyses. The primary analysis showed that one cluster was significant at the FDR-threshold (RC 8), while two others were significant prior to FDR thresholding (RC 7 and RC 5). Given the novelty of these brainstem examinations and the non-specific summary measure of the primary analysis (potentially obscuring more specific relations), we also examined follow-up analyses in the two clusters that were significant prior to the FDR-threshold. Therefore, we performed correlations with the three brainstem clusters in association with the SRS-2 subscores of social awareness, social cognition, social motivation, social communication, and repetitive behaviors, the SCQ total score (as this measure does not have subscores), and the RBS-R subscores of stereotyped, self-injurious, compulsive, ritualistic, sameness, and restricted behaviors (log-transformed for normality). As in the primary analyses, these analyses controlled for age, sex, and head motion and were FDR-corrected. To examine a potential moderating effect of age, follow-up regression analyses examined the impact of age on the relation between the summary measures of autism features and the brainstem clusters found in the primary analysis, while also controlling for sex and head motion. Because 39% of the autistic children in the sample were taking a centrally active medication, follow-up analyses also examined the impact of medication status on the relation between the summary measures of autism features and the brainstem clusters found in the primary analysis.
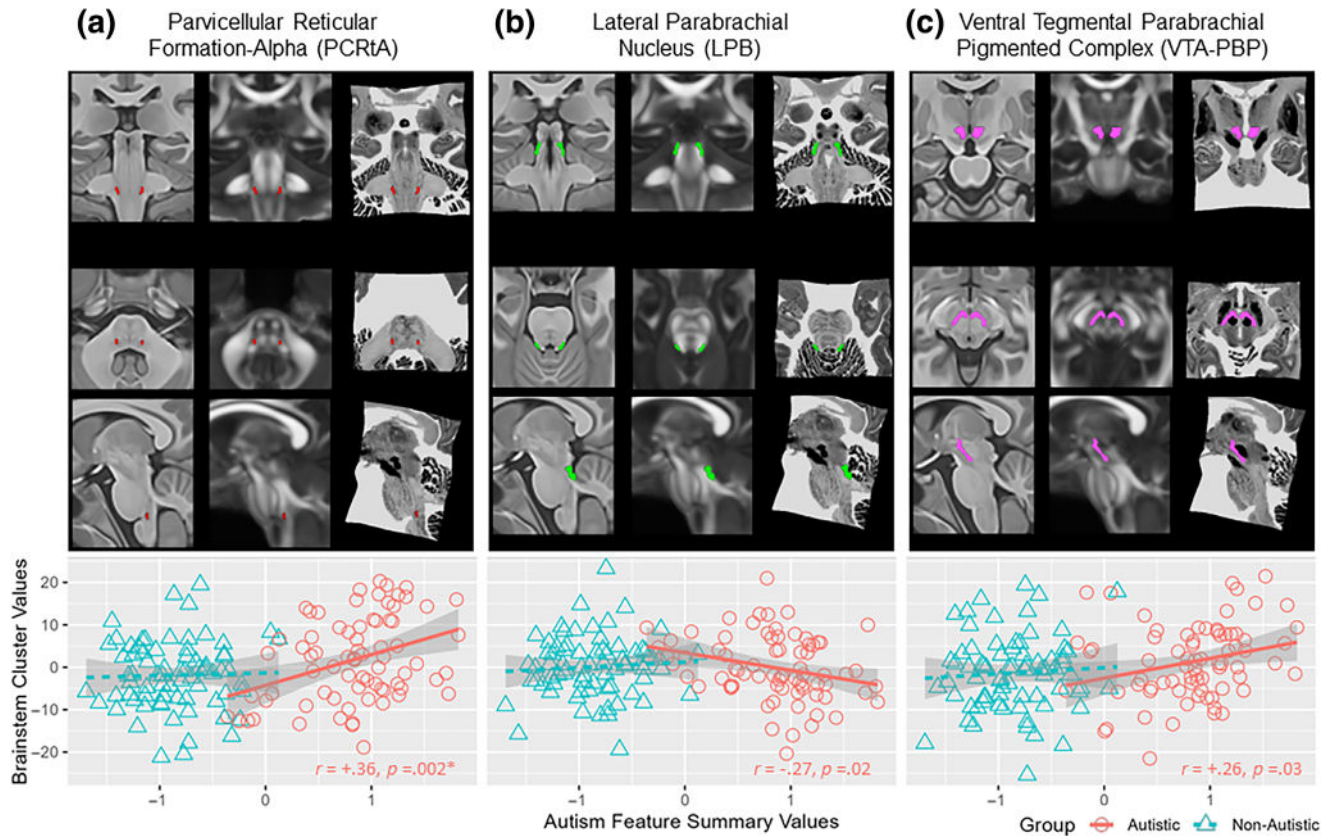
FIGURE 1 Anatomical locations of brainstem clusters and correlations with autism features. Panel (a) shows brainstem cluster 8 (RC8), primarily representing the bilateral parvicellular reticular formation-alpha (PCRtA). Panel (b) shows brainstem cluster 7 (RC7), primarily representing the bilateral lateral parabrachial nucleus (LPB). Panel (c) shows brainstem cluster 5 (RC5), primarily representing the bilateral ventral tegmental parabrachial pigmented complex (VTA-PBP). To be able to show their precise location, the brainstem nuclei are shown on the T1-weighted structural population image, the fractional anisotropy (FA) population image, and on a publicly available histology image mapped into our data space (Amunts et al., 2013; Sitek et al., 2019). Within the autism group, individual differences in autism features showed moderate-sized, significant correlations with the PCRtA cluster (RC8), but small-sized correlations that did not meet the FDR-corrected thresholds with the LPB (RC7) and VTA-PBP (RC 5). All brainstem cluster values and autism feature values were mean-centered and residualized for age, sex, and head motion for correlations and scatterplots. *denotes significance at the level of $p < 0.05$ FDR-corrected.

Replication analyses

Given the novelty of this investigation, we sought to independently replicate the findings in a previously collected dataset of 24 autistic and 21 non-autistic adolescents (13.0–17.9 years of age). Details of these participants can be found in Table S2. While these data were not collected using brainstem-optimized imaging, we applied the TiDi-Fused processing pipeline to enhance the accuracy of the brainstem images through post-processing (see Figure S14). We replicated clusters RC8 (PCRtA), RC7 (LPB), and RC5 (VTA-PBP) by performing three separate PCA's: one for the bilateral PCRtA, one for the bilateral LPB, and one for the bilateral VTA-PBP (see Supporting Information Methods for details and Tables S3–S5 for rotational loadings for each replicated cluster). Due to the smaller size of this replication sample, percentage bend robust correlations (Mair & Wilcox, 2019) were performed, controlling for

age, sex, and head motion. These analyses were performed within the autistic group and then across the combined group.

RESULTS

Among all the brainstem clusters (RC1 through RC13), primary analyses demonstrated a significant ($p < 0.05$, FDR-corrected) and moderate-sized correlation between the autism-features summary measure and the bilateral PCRtA cluster (RC8), both within the autistic group and across the whole sample (Figure 1, Table 2, Figure S15). Specifically, more pronounced autistic features were associated with a summary measure that primarily reflected decreased FA and AD and increased RD and ODI of this bilateral cluster (see Table S1 for factor loadings). Two other clusters (RC7, primarily reflecting bilateral LPB FA, MD, RD, ICVF, and ODI, and RC5, primarily

TABLE 2 Brainstem cluster correlations with autism-features summary measure within autism group and in the combined autism and non-autism groups.

| Brainstem cluster	Autism group (n = 74)		Combined autism and non-autism group (n = 145)	
	Pearson R	p-Value	Pearson R	p-Value
RC1	+0.05	0.67	+0.13	0.12
RC2	−0.18	0.13	−0.19	0.02
RC3	+0.03	0.80	+0.08	0.31
RC4	+0.06	0.61	−0.08	0.32
RC5	+0.26	0.03	+0.22	0.009
RC6	+0.02	0.87	+0.19	0.02
RC7	−0.27	0.02	−0.07	0.42
RC8	+0.36	0.002*	+0.29	0.0005*
RC9	−0.10	0.41	−0.09	0.26
RC10	−0.10	0.40	−0.17	0.04
RC11	+0.02	0.86	+0.13	0.12
RC12	+0.18	0.12	+0.05	0.56
RC13	−0.12	0.32	−0.17	0.04

*$p < 0.05$ fdr-corrected.
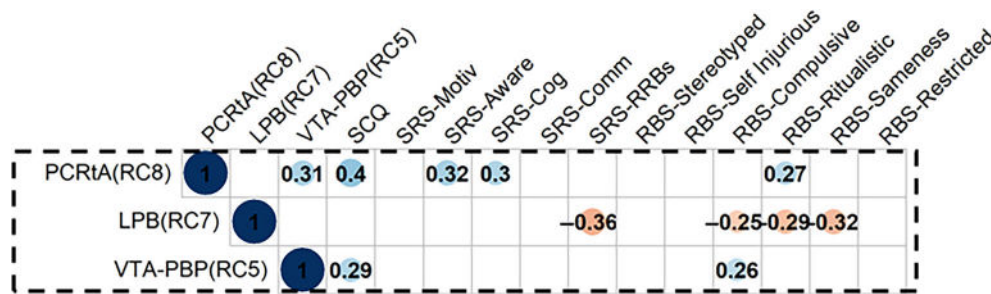
FIGURE 2 Follow-up *Pearson R* correlations with specific autism-feature measures. The dashed-line box highlights the associations with the brainstem clusters of interest. Correlation values are shown if they met significance at the level of $p < 0.05$ FDR-corrected. The parvicellular reticular formation-alpha (PCRtA) cluster (RC8) showed moderate-sized correlations with the Social Communication Questionnaire (SCQ) (Rutter, Bailey, & Lord, 2003) total score and with the Social Responsiveness Score, Second Edition (SRS-2) (Constantino & Gruber, 2012) awareness and cognitive domains, while showing small-sized correlations with the Repetitive Behavior Scale-Revised (RBS-R) (Bodfish et al., 1999) ritualistic domain. The LPB cluster (RC7) showed moderate-sized correlations with the SRS-2 repetitive and restricted behavior domain (RRBs), and small sized correlations with the RBS-R compulsive, ritualistic, and sameness domains. The VTA-PBP (RC5) cluster showed small-sized correlations with SCQ total score and the RBS-R compulsive domain. All brainstem cluster values and autism feature values were residualized for age, sex, and head motion for this analysis.

reflecting bilateral VTA-PBP AD, MD, RD, ICVF, and ODI and PAG AD and ICVF) had small-sized relations with autism features but only at the $p < 0.05$ uncorrected threshold. Specifically, for the LPB cluster (RC7), more pronounced autism features were associated with decreased MD, RD, ICVF, and ODI and increased FA. For the VTA-PBP cluster (RC5), more pronounced autism features were associated with increased AD, RD, MD and decreased ODI.

Follow-up analyses within the autistic group (Figure 2) demonstrated that the PCRtA cluster (RC8) was associated with SCQ, SRS awareness, SRS cognition, and RBS-R ritualistic scores ($p < 0.05$ FDR-corrected). The LPB cluster was associated with SRS-2 repetitive behaviors, RBS-R compulsive, RBS-R

ritualistic, and RBS-R sameness scores ($p < 0.05$ FDR-corrected). The VTA-PBP cluster was associated with SCQ and RBS-R compulsive scores ($p < 0.05$ FDR-corrected).

Follow-up age regression analyses did not find significant age-by-autism-feature interaction effects for the PCRtA (RC8), $b = -0.63$, SE $= 1.62$, $t = -0.39$, $p = 0.70$, for the LPB (RC7), $b = -1.72$, SE $= 1.25$, $t = -1.38$, $p = 0.17$, nor for the VTA-PBP (RC5), $b = -0.41$, SE $= 1.47$, $t = -0.28$, $p = 0.78$.

Follow-up medication status analyses (Figure 3) found large-sized correlations between autism features and PCRtA (RC8), $r = +0.52$, $p = 0.004$, and LPB (RC7), $r = -0.50$, $p = 0.006$, in the autistic participants (n = 29) who were taking a psychotropic medication at
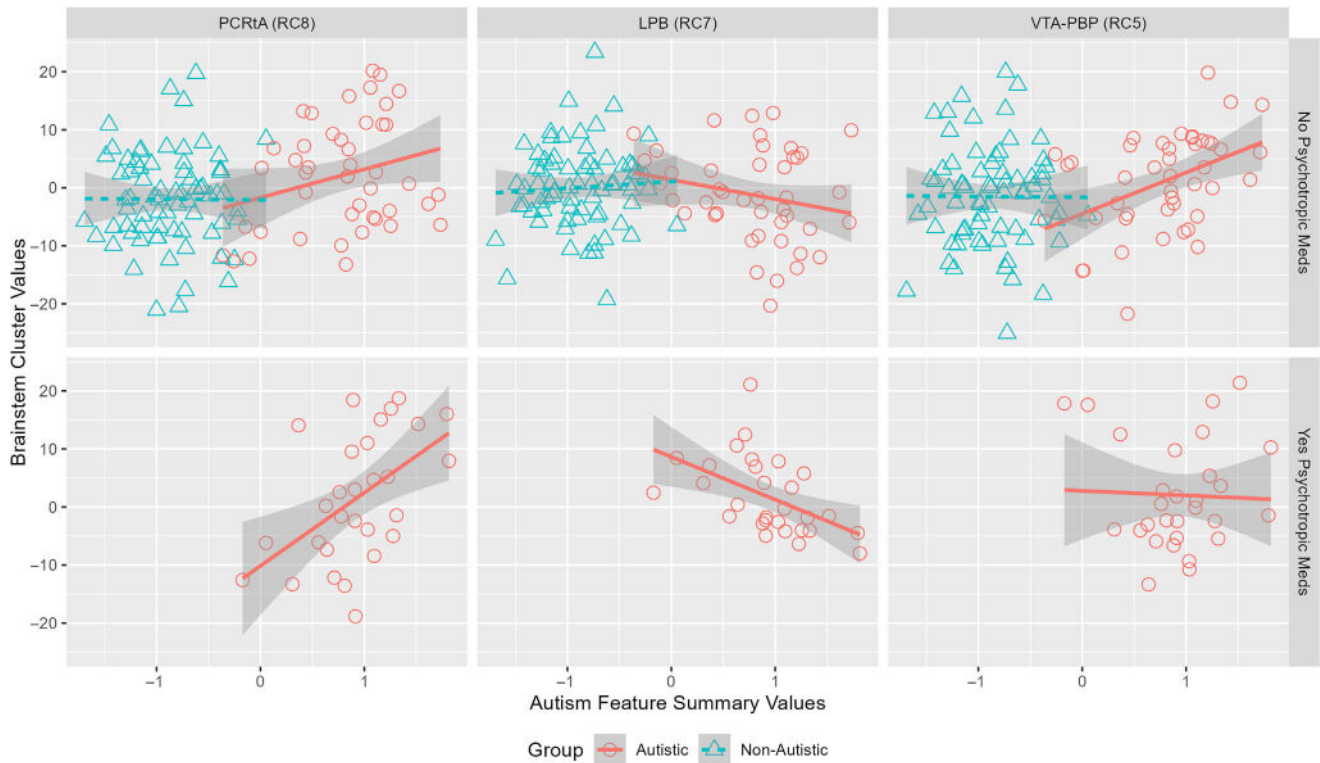
FIGURE 3 Follow-up examination of centrally active, psychotropic medication use. Scatterplots show how current medication status impacts the correlations between the brainstem clusters of interest and autism summary features. The only significant moderation effect was with the VTA-PBP. Brainstem cluster 8 (RC8), primarily represents the bilateral parvicellular reticular formation-alpha (PCRtA), brainstem cluster 7 (RC7) primarily represents the bilateral lateral parabrachial nucleus (LPB), and brainstem cluster 5 (RC5) primarily represents the bilateral ventral tegmental parabrachial pigmented complex (VTA-PBP). All brainstem cluster values and autism feature values were mean-centered and residualized for age, sex, and head motion for correlations and scatterplots.

the time of the study, but small-sized correlations in the autistic participants ($n = 45$) who were not taking a psychotropic medication, $r = +0.27$, $p = 0.07$, $r = -0.22$, $p = 0.16$. respectively. The difference in these correlations as a function of medication status was not statistically significant, PCRtA: $p = 0.86$ and LPB: $p = 0.21$, suggesting that even though the descriptive magnitude of these relationships were different, there was not a statistical difference between these correlations in the children who were taking psychotropic medication and not taking psychotropic medication. In contrast, the VTA-PBP cluster (RC5) showed a statistically significant interaction effect, $p = 0.03$, with medium-to-large sized correlation in the autistic participants who were not taking a psychotropic medication at the time of the study, $r = +0.44$, $p = 0.002$, but virtually no correlation in those who were taking a psychotropic medication, $r = -0.05$, $p = 0.83$.

Results of the robust correlation analyses in the replication sample can be seen in Table 3. The replicated PCRtA cluster was associated with SCQ and SRS-2 awareness scores within the autistic adolescents and across the autistic and non-autistic-combined adolescent sample, but not the SRS-2 cognition and RBS-R ritualistic scores. The replicated LPB cluster was found to relate to the RBS-R sameness score in the full replication

sample of autistic and non-autistic individuals but not within the autism replication sample alone. None of the VTA-PBP replication correlations were significant.

Like the primary analyses, follow-up age regression analyses in the replication sample did not find significant age-by-autism-feature interaction effects for the PCRtA (RC8), the LPB (RC7), nor the VTA-PBP (RC5) (see Table S6). However, because these interaction follow-up analyses in the replication dataset are likely underpowered, we graphed the three (of 10) interaction effects that had p-values <0.20 (Figure S16). From these graphs, two of the interaction effects (LBP with SRS-2 RRBs and VTA-PBP with SCQ) suggested trending stronger correlations in the younger participants (i.e., <15.8 years, median age of sample), whereas one interaction effect (VTA-PBP and RBS-R Compulsive) suggested trending stronger correlation in the older participants (i.e., those older than 15.8 years-old).

DISCUSSION

The present study set out to characterize how the microstructural properties of autonomic, pain, and limbic brainstem nuclei relate to individual variation in core

TABLE 3 Robust correlation replication analyses in smaller, adolescent sample with improved processing but without improved imaging acquisition.

	Autistic sample		Autistic and non-autistic combined sample	
	Robust correlation	*p*-Value	Robust correlation	*p*-Value
PCRtA cluster				
SCQ	+0.45	0.03	+0.31	0.04
SRS-awareness	+0.41	<0.05	+0.34	0.02
SRS-cognition	+0.14	0.52	+0.19	0.22
RBS-R ritualistic	+0.26	0.22	+0.21	0.16
LPB cluster				
SRS-2 RRBs	+0.01	0.96	−0.24	0.11
RBS-R compulsive	−0.26	0.23	−0.28	0.07
RBS-R ritualistic	−0.21	0.33	−0.29	0.05
RBS-R sameness	−0.16	0.46	−0.36	0.01
VTA-PBP				
SCQ	−0.21	0.33	−0.13	0.39
RBS-R compulsive	+0.15	0.47	+0.09	0.55

social and repetitive behavior features in autistic children. Consistent with theories that suggest that brainstem nuclei relate to core autism features, the findings highlighted three specific reticular formation nuclei of interest: the PCRtA, LPB, and VTA-PBP. The most robust finding was the PCRtA's relation with social communication and social awareness measures, which was replicated in an independent sample of adolescents. A secondary finding was the LPB's relation with repetitive behaviors (particularly insistence on sameness) in the childhood sample, but this finding was only partially replicated in the independent sample of adolescents (i.e., only found in the combined autistic and non-autistic replication sample). Moreover, the VTA-PBP was found to have small-sized associations with the autism summary measure, but none of the small-sized associations were replicated. Taken together, these results suggest that the PCRtA is related to the social communication aspect of autistic features, whereas the LPB may be primarily associated with repetitive behavior features. Given the very few studies that have examined the PCRtA in humans (Cauzzo et al., 2022; Singh et al., 2022) and the relatively little animal-model research into the PCRtA, it is unclear how the PCRtA facilitates social behaviors. However, we discuss our findings below in reference to what we know about PCRtA anatomy, connections, and functions.

Located at the junction of the pons and the medulla of the brainstem and adjacent to the nucleus ambiguous (a key nucleus in the polyvagal theory; Porges, 2003, 2005), the PCRtA in animal models is known to be widely interconnected with structures throughout the brain, such as the nearby trigeminal nuclei, other brainstem nuclei (including the parabrachial complex and the locus coeruleus), the thalamus, amygdala, hypothalamus, and deep cerebellar nuclei (Shammah-Lagnado

et al., 1992). Similar PCRtA tract-based projections recently have been found in humans (Singh et al., 2022), and functional connectivity was also observed between the PCRtA and other brainstem nuclei, the cerebellum, and the basal ganglia (Cauzzo et al., 2022). This abundant pattern of connections implies that the PCRtA may be a key part of brain-wide networks involved in motor and autonomic functions. Mapping and comparing these PCRtA-involved regions at the network level in autistic and non-autistic individuals will be a key next step of future research to better understand how the PCRtA and its connected brain regions may further elucidate the role of the PCRtA in social communication.

In terms of functions, the PCRtA is known to be involved in oromotor functions and cardio-respiration in animal models (Shammah-Lagnado et al., 1992). The PCRtA's oromotor functions include swallowing (Cunningham & Sawchenko, 2000), chewing (Shammah-Lagnado et al., 1992), licking (Travers et al., 1997), salivation (Ramos & Puerto, 1988), and abdominal organ metabolic homeostasis (Ter Horst et al., 1991). As such, we speculate that the PCRtA could be associated with the high prevalence of feeding and gastro-intestinal differences in autistic individuals (Mayes & Zickgraf, 2019), which is a key area for future research. The PCRtA is also known to play a role in autonomic functioning, likely through its connections with the hypothalamus and amygdala. Specifically, the PCRtA is thought to be involved in cardiovascular changes that occur in response to defense-alerting mechanisms (Yadid & Friedman, 2008) and acts that require interruptions or changes in respiration, such as sneezing (Krishnan et al., 2007) and swallowing (Car & Amri, 1982) (as reviewed by Shammah-Lagnado et al., 1992). These functions are in line with autistic behaviors that led to the

original theories implicating the reticular formation in autism (Hutt et al., 1964; Rimland, 1964), However, future research will need to examine behavioral indices of autonomic functions in light of PCRtA structure in order to better understand this brain-behavior relationship and its potential contributions to social communication differences.

In addition to the PCRtA findings, two aspects of the parabrachial network, the LPB and VTA-PBP, were not as robustly related to core autism features but may nonetheless be important brainstem areas for future investigations. The VTA-PBP (located in the midbrain) was found to have small associations with SCQ, social cognition, and compulsive behaviors and is known to be involved in motivated behaviors, aversion, reward, and depression (Chaudhury et al., 2013; Friedman et al., 2008, 2009; Krishnan et al., 2007; Lammel et al., 2014; Yadid & Friedman, 2008). In contrast, the LPB is known to be involved in visceral nociception, as a key part of the pain network (Hermanson & Blomqvist, 1996; Sun et al., 2020). The LPB (located in the caudal pons) was found to have small-to-moderate associations with repetitive behaviors, particularly insistence on sameness and adherence to routines. This link brings up the possibility that routinized behaviors in autism may be related to neural pain networks. Intriguingly, the LPB values had the inverse relationship to autism features than the PCRtA and VTA-PBP, suggesting that similar brainstem nuclei properties may have different impacts on autism features based on the specific nucleus. Future investigations into the structural properties of the connections among these nuclei may elucidate what is underlying this pattern of results, as we know that the PCRtA, LPB, and VTA-PBP are interconnected and are also each connected to the amygdala, thalamus, and hypothalamus.

While it is a strength of the study that we sought to replicate our findings using an independent dataset, it is important to note the differences between our original and replication samples. Specifically, our replication sample was a smaller sample of adolescents and included imaging processing, but not acquisition parameters, that would enhance brainstem images. The differences between the original and replication samples make the replication of the PCRtA findings even more striking, but future replication in larger samples with brainstem-optimized images is desirable. Moreover, because of the developmental nature of autism, age is likely an impactful variable in this line of research, making the age differences in the original and replication samples notable. While we did not observe a moderating impact of age on the relationships between brainstem cluster values and autism features, some trending interaction effects in the replication sample suggested that future studies should examine whether these brainstem-behavior relationships persist across all ages or if they might be age-specific. Another difference between the original and replication datasets was the medication status of the autistic

participants, with only 39% of the original sample but 63% of the replication sample being on a psychotropic medication. These sample differences reflect previous findings that older autistic children and adolescents are more likely than younger autistic children to be treated with psychotropic medication (Mire et al., 2015). Our results found that medication status moderated the VTA-PBP findings, such that the relationship between autism features and brainstem microstructure was only present in autistic children who were not taking a psychotropic medication. Therefore, it is possible that the VTA-PBP was not replicated because of the high percentage of autistic adolescents in the replication sample currently taking medication. As such, it is important to examine the impact of psychotropic medication on the VTA-PBP in future studies with even larger sample sizes.

The present findings should also be interpreted in consideration of study limitations. To be able to continue this research during the COVID-19 pandemic, this study's diagnostic procedures changed, making it such that we only had caregiver-reported measures (and not observed measures) of autism features across the entire sample. Future studies should examine these findings in light of ADOS-2 scores. Additionally, participants in this study were 6.0–10.9 years-old, communicated through spoken language with our study team, and were able to acclimate to the MRI environment, which should be considered when evaluating the generalizability of these findings to the whole of the autism spectrum. Moreover, autism is a heterogeneous condition likely made up of multiple distinct conditions (Cohen et al., 1986; Xavier et al., 2015). While the analyses here examined how individual differences in autism features related to microstructure of brainstem regions, it is likely that these features do not fall on a single continuum. Future research with larger samples would benefit from cluster analyses that could examine potential autism subgroups. Finally, previous research has shown adequate translation of this brainstem atlas from 7T-scanner data to 3T-scanner data (Singh et al., 2022). However, these brainstem nuclei are small, and it is possible that biologically distinct but adjacent areas like the PCRtA and nucleus ambiguous may have been structurally indistinguishable. While we believe our combined brainstem-optimized imaging and TiDi-Fused processing is a good start, future optimization of brainstem MRI is needed to continue to enhance resolution while still allowing for scan times that are feasible for pediatric imaging. In parallel, human tissue analysis is needed to replicate and confirm these MRI findings in order to provide a more microscopic view of these very small brainstem nuclei, their connections, and the complexity of the different types of neurons that make up these brainstem regions.

In all, this study set out to test 60-year-old theories that the brainstem's reticular formation is associated with autism features (Hutt et al., 1964; Rimland, 1964) using

methods to enhance brainstem imaging and image-processing in autistic children. We found specific autonomic, limbic, and nociceptive nuclei, most robustly the PCRtA but to a lesser degree the LPB, to be associated with autism features. Moreover, the present study suggested a split among these nuclei, such that the PCRtA was most robustly associated with social communication behaviors, whereas the LPB was most robustly associated with the insistence-on-sameness aspect of repetitive behaviors. The results also suggest that the VTA-PBP may be a nucleus of interest for future investigations. Given that these nuclei are highly connected with each other, other brainstem nuclei, the thalamus, amygdala, cerebellum, and other cortical regions, understanding the pattern of connections among these nuclei at the network level and in relation to autism features will be a key future direction.

DATA AVAILABILITY STATEMENT

The data that support the findings of this study are openly available in NIMH Data Archive at http://doi.org/10.15154/1528987, reference number 2131.

ETHICAL STATEMENT

All study procedures and documents conform to the standards of the Declaration of Helsinki and were approved by the University of Wisconsin-Madison Health Sciences Institutional Review Board (IRB #2018-1067).

ORCID

Brittany G. Travers https://orcid.org/0000-0002-8161-3858

REFERENCES

American Psychiatric Association. (2013). *Diagnostic and statistical manual of mental disorders* (Fifth ed.). American Psychiatric Association. https://doi.org/10.1176/appi.books.9780890425596

Amunts, K., Lepage, C., Borgeat, L., Mohlberg, H., Dickscheid, T., Rousseau, M. É., Bludau, S., Bazin, P. L., Lewis, L. B., Oros-Peusquens, A. M., Shah, N. J., Lippert, T., Zilles, K., & Evans, A. C. (2013). BigBrain: An ultrahigh-resolution 3D human brain model. *Science*, *340*, 1472–1475. https://doi.org/10.1126/science.1235381

Andersson, J. L. R., Graham, M. S., Drobnjak, I., Zhang, H., Filippini, N., & Bastiani, M. (2017). Towards a comprehensive framework for movement and distortion correction of diffusion MR images: Within volume movement. *NeuroImage*, *152*, 450–466. https://doi.org/10.1016/j.neuroimage.2017.02.085

Andersson, J. L. R., Graham, M. S., Zsoldos, E., & Sotiropoulos, S. N. (2016). Incorporating outlier detection and replacement into a non-parametric framework for movement and distortion correction of diffusion MR images. *NeuroImage*, *141*, 556–572. https://doi.org/10.1016/j.neuroimage.2016.06.058

Andersson, J. L. R., Skare, S., & Ashburner, J. (2003). How to correct susceptibility distortions in spin-echo echo-planar images: Application to diffusion tensor imaging. *NeuroImage*, *20*(2), 870–888. https://doi.org/10.1016/S1053-8119(03)00336-7

Andersson, J. L. R., & Sotiropoulos, S. N. (2016). An integrated approach to correction for off-resonance effects and subject movement in diffusion MR imaging. *NeuroImage*, *125*, 1063–1078. https://doi.org/10.1016/j.neuroimage.2015.10.019

Arora, I., Bellato, A., Ropar, D., Hollis, C., & Groom, M. J. (2021). Is autonomic function during resting-state atypical in Autism: A systematic review of evidence. *Neuroscience and Biobehavioral Reviews*, *125*, 417–441. https://doi.org/10.1016/j.neubiorev.2021.02.041

Avants, B. B., Tustison, N. J., Song, G., Cook, P. A., Klein, A., & Gee, J. C. (2011). A reproducible evaluation of ANTs similarity metric performance in brain image registration. *NeuroImage*, *54*(3), 2033–2044. https://doi.org/10.1016/j.neuroimage.2010.09.025

Avants, B. B., Tustison, N. J., Wu, J., Cook, P. A., & Gee, J. C. (2011). An open source multivariate framework for n-tissue segmentation with evaluation on public data. *Neuroinformatics*, *9*(4), 381–400. https://doi.org/10.1007/s12021-011-9109-y

Bastiani, M., Cottaar, M., Fitzgibbon, S. P., Suri, S., Alfaro-Almagro, F., Sotiropoulos, S. N., Jbabdi, S., & Andersson, J. L. R. (2019). Automated quality control for within and between studies diffusion MRI data using a non-parametric framework for movement and distortion correction. *NeuroImage*, *184*, 801–812. https://doi.org/10.1016/j.neuroimage.2018.09.073

Benevides, T. W., & Lane, S. J. (2015). A review of cardiac autonomic measures: Considerations for examination of physiological response in children with autism spectrum disorder. *Journal of Autism and Developmental Disorders*, *45*(2), 560–575. https://doi.org/10.1007/s10803-013-1971-z

Benjamini, Y., & Hochberg, Y. (1995). Controlling the false discovery rate: A practical and powerful approach to multiple testing. *Journal of the Royal Statistical Society: Series B (Methodological)*, *57*(1), 289–300.

Bianciardi, M., Strong, C., Toschi, N., Edlow, B. L., Fischl, B., Brown, E. N., Rosen, B. R., & Wald, L. L. (2018). A probabilistic template of human mesopontine tegmental nuclei from in vivo 7T MRI. *NeuroImage*, *170*, 222–230. https://doi.org/10.1016/j.neuroimage.2017.04.070

Bianciardi, M., Toschi, N., Edlow, B. L., Eichner, C., Setsompop, K., Polimeni, J. R., Brown, E. N., Kinney, H. C., Rosen, B. R., & Wald, L. L. (2015). Toward an in vivo neuroimaging template of human brainstem nuclei of the ascending arousal, autonomic, and motor systems. *Brain Connectivity*, *5*(10), 597–607. https://doi.org/10.1089/brain.2015.0347

Bodfish, J. W., Symons, F. J., Parker, D. E., & Lewis, M. H. (1999). Repetitive behavior scale: Test manual. *Western Carolina Center Research Reports*.

Bosco, P., Giuliano, A., Delafield-Butt, J., Muratori, F., Calderoni, S., & Retico, A. (2019). Brainstem enlargement in preschool children with autism: Results from an intermethod agreement study of segmentation algorithms. *Human Brain Mapping*, *40*(1), 7–19. https://doi.org/10.1002/hbm.24351

Burstein, O., & Geva, R. (2021). The brainstem-informed autism framework: Early life neurobehavioral markers. *Frontiers in Integrative Neuroscience*, *15*, 759614. https://doi.org/10.3389/fnint.2021.759614

Car, A., & Amri, M. (1982). Etude des neurones deglutiteurs pontiques chez la brebis: I. Activite et localisation. *Experimental Brain Research*, *48*, 345–354.

Casado-Sainz, A., Gudmundsen, F., Baerentzen, S. L., Lange, D., Ringsted, A., Martinez-Tejada, I., Medina, S., Lee, H., Svarer, C., Keller, S. H., Schain, M., Kjaerby, C., Fisher, P. M., Cumming, P., & Palner, M. (2022). Dorsal striatal dopamine induces fronto-cortical hypoactivity and attenuates anxiety and compulsive behaviors in rats. *Neuropsychopharmacology*, *47*, 454–464. https://doi.org/10.1038/s41386-021-01207-y

Cauzzo, S., Singh, K., Stauder, M., García-Gomar, M. G., Vanello, N., Passino, C., Staab, J., Indovina, I., & Bianciardi, M. (2022). Functional connectome of brainstem nuclei involved in autonomic, limbic, pain and sensory processing in living humans from 7 Tesla resting state fMRI. *NeuroImage*, *250*, 118925. https://doi.org/10.1016/j.neuroimage.2022.118925

Chaudhury, D., Walsh, J. J., Friedman, A. K., Juarez, B., Ku, S. M., Koo, J. W., Ferguson, D., Tsai, H.-C., Pomeranz, L., Christoffel, D. J., Nectow, A. R., Ekstrand, M., Domingos, A., Mazei-Robison, M. S., Mouzon, E., Lobo, M. K., Neve, R. L., Friedman, J. M., Russo, S. J., … Han, M.-H. (2013). Rapid regulation of depression-related behaviours by control of midbrain dopamine neurons. *Nature*, *493*(7433), 532–536. https://doi.org/10.1038/nature11713

Cohen, D. J., Volkmar, F. R., & Paul, R. (1986). Introduction: Issues in the classification of pervasive developmental disorders: History and current status of nosology. *Journal of the American Academy of Child Psychiatry*, *25*(2), 158–161. https://doi.org/10.1016/S0002-7138(09)60221-1

Constantino, J., & Gruber, C. (2012). *Social responsiveness scale-second edition (SRS-2)*. Western Psychological Services.

Cormen, T. H., & Cormen, T. H. (Eds.). (2001). *Introduction to algorithms* (2nd ed.). MIT Press.

Cunningham, E. T., Jr., & Sawchenko, P. E. (2000). Dorsal medullary pathways subserving oromotor reflexes in the rat: Implications for the central neural control of swallowing. *Journal of Comparative Neurology*, *417*(4), 448–466.

Cuve, H. C., Gao, Y., & Fuse, A. (2018). Is it avoidance or hypoarousal? A systematic review of emotion recognition, eye-tracking, and psychophysiological studies in young adults with autism spectrum conditions. *Research in Autism Spectrum Disorders*, *55*, 1–13.

Dadalko, O. I., & Travers, B. G. (2018). Evidence for brainstem contributions to autism spectrum disorders. *Frontiers in Integrative Neuroscience*, *12*, 47. https://doi.org/10.3389/fnint.2018.00047

Delafield-Butt, J., & Trevarthen, C. (2018). On the brainstem origin of autism: Disruption to movements of the primary self. In *Autism* (pp. 119–138). CRC Press.

Dick, F., Tierney, A. T., Lutti, A., Josephs, O., Sereno, M. I., & Weiskopf, N. (2012). In vivo functional and myeloarchitectonic mapping of human primary auditory areas. *The Journal of Neuroscience*, *32*(46), 16095–16105. https://doi.org/10.1523/JNEUROSCI.1712-12.2012

DiPiero, M. A., Surgent, O. J., Travers, B. G., Alexander, A. L., Lainhart, J. E., & Dean, D. C. (2023). Gray matter microstructure differences in autistic males: A gray matter based spatial statistics study. *NeuroImage Clinical*, *37*, 103306. https://doi.org/10.1016/j.nicl.2022.103306

Edgeworth, F. Y. (1887). On observations relating to several quantities. *Hermathena*, *6*(13), 279–285.

Edgeworth, F. Y. (1888). XXII. On a new method of reducing observations relating to several quantities. *The London, Edinburgh, and Dublin Philosophical Magazine and Journal of Science*, *25*(154), 184–191. https://doi.org/10.1080/14786448808628170

Fernández, M., Mollinedo-Gajate, I., & Peñagarikano, O. (2018). Neural circuits for social cognition: Implications for autism. *Neuroscience*, *370*, 148–162. https://doi.org/10.1016/j.neuroscience.2017.07.013

Fick, R. H. J., Wassermann, D., & Deriche, R. (2019). The Dmipy Toolbox: Diffusion MRI multi-compartment modeling and microstructure recovery made easy. *Frontiers in Neuroinformatics*, *13*, 64. https://doi.org/10.3389/fninf.2019.00064

Friedman, A., Frankel, M., Flaumenhaft, Y., Merenlender, A., Pinhasov, A., Feder, Y., Taler, M., Gil-Ad, I., Abeles, M., & Yadid, G. (2009). Programmed acute electrical stimulation of ventral tegmental area alleviates depressive-like behavior. *Neuropsychopharmacology*, *34*(4), 1057–1066. https://doi.org/10.1038/npp.2008.177

Friedman, A., Friedman, Y., Dremencov, E., & Yadid, G. (2008). VTA dopamine neuron bursting is altered in an animal model of depression and corrected by desipramine. *Journal of Molecular Neuroscience*, *34*(3), 201–209. https://doi.org/10.1007/s12031-007-9016-8

García-Gomar, M. G., Strong, C., Toschi, N., Singh, K., Rosen, B. R., Wald, L. L., & Bianciardi, M. (2019). In vivo probabilistic structural atlas of the inferior and superior colliculi, medial and lateral geniculate nuclei and superior olivary complex in humans based on 7 Tesla MRI. *Frontiers in Neuroscience*, *13*, 764. https://doi.org/10.3389/fnins.2019.00764

García-Gomar, M. G., Videnovic, A., Singh, K., Stauder, M., Lewis, L. D., Wald, L. L., Rosen, B. R., & Bianciardi, M. (2022). Disruption of brainstem structural connectivity in rem sleep behavior disorder using 7 Tesla magnetic resonance imaging. *Movement Disorders*, *37*(4), 847–853. https://doi.org/10.1002/mds.28895

Greve, D. N., & Fischl, B. (2009). Accurate and robust brain image alignment using boundary-based registration. *NeuroImage*, *48*(1), 63–72. https://doi.org/10.1016/j.neuroimage.2009.06.060

Guerrero-Gonzalez, J., Surgent, O., Adluru, N., Kirk, G. R., Dean Iii, D. C., Kecskemeti, S. R., Alexander, A. L., & Travers, B. G. (2022). Improving imaging of the brainstem and cerebellum in autistic children: Transformation-based high-resolution diffusion MRI (TiDi-fused) in the human brainstem. *Frontiers in Integrative Neuroscience*, *16*, 804743. https://doi.org/10.3389/fnint.2022.804743

Hermanson, O., & Blomqvist, A. (1996). Subnuclear localization of FOS-like immunoreactivity in the rat parabrachial nucleus after nociceptive stimulation. *The Journal of Comparative Neurology*, *368*(1), 45–56. https://doi.org/10.1002/(SICI)1096-9861(19960422)368:1<45::AID-CNE4>3.0.CO;2-K

Hoy, A. R., Koay, C. G., Kecskemeti, S. R., & Alexander, A. L. (2014). Optimization of a free water elimination two-compartment model for diffusion tensor imaging. *NeuroImage*, *103*, 323–333. https://doi.org/10.1016/j.neuroimage.2014.09.053

Hutt, C., Hutt, S. J., Lee, D., & Ounsted, C. (1964). Arousal and childhood autism. *Nature*, *204*, 908–909. https://doi.org/10.1038/204908a0

Irfanoglu, M. O., Modi, P., Nayak, A., Hutchinson, E. B., Sarlls, J., & Pierpaoli, C. (2015). DR-BUDDI (Diffeomorphic Registration for Blip-Up blip-Down Diffusion Imaging) method for correcting

echo planar imaging distortions. *NeuroImage*, *106*, 284–299. https://doi.org/10.1016/j.neuroimage.2014.11.042

Irfanoglu, M. O., Walker, L., Sarlls, J., Marenco, S., & Pierpaoli, C. (2012). Effects of image distortions originating from susceptibility variations and concomitant fields on diffusion MRI tractography results. *NeuroImage*, *61*(1), 275–288. https://doi.org/10.1016/j.neuroimage.2012.02.054

Jou, R. J., Minshew, N. J., Melhem, N. M., Keshavan, M. S., & Hardan, A. Y. (2009). Brainstem volumetric alterations in children with autism. *Psychological Medicine*, *39*(8), 1347–1354. https://doi.org/10.1017/S0033291708004376

Kecskemeti, S., & Alexander, A. L. (2020a). Three-dimensional motion-corrected T1 relaxometry with MPnRAGE. *Magnetic Resonance in Medicine*, *84*(5), 2400–2411. https://doi.org/10.1002/mrm.28283

Kecskemeti, S., Freeman, A., Travers, B. G., & Alexander, A. L. (2021). FreeSurfer based cortical mapping and T1-relaxometry with MPnRAGE: Test-retest reliability with and without retrospective motion correction. *NeuroImage*, *242*, 118447. https://doi.org/10.1016/j.neuroimage.2021.118447

Kecskemeti, S., Samsonov, A., Hurley, S. A., Dean, D. C., Field, A., & Alexander, A. L. (2016). MPnRAGE: A technique to simultaneously acquire hundreds of differently contrasted MPRAGE images with applications to quantitative T1 mapping. *Magnetic Resonance in Medicine*, *75*(3), 1040–1053. https://doi.org/10.1002/mrm.25674

Kecskemeti, S., Samsonov, A., Velikina, J., Field, A. S., Turski, P., Rowley, H., … Alexander, A. L. (2018). Robust motion correction strategy for structural MRI in unsedated children demonstrated with three-dimensional radial MPnRAGE. *Radiology*, *289*(2), 509–516. https://doi.org/10.1148/radiol.2018180180

Kecskemeti, S. R., & Alexander, A. L. (2020b). Test-retest of automated segmentation with different motion correction strategies: A comparison of prospective versus retrospective methods. *NeuroImage*, *209*, 116494. https://doi.org/10.1016/j.neuroimage.2019.116494

Kellner, E., Dhital, B., Kiselev, V. G., & Reisert, M. (2016). Gibbs-ringing artifact removal based on local subvoxel-shifts. *Magnetic Resonance in Medicine*, *76*(5), 1574–1581. https://doi.org/10.1002/mrm.26054

Krishnan, V., Han, M.-H., Graham, D. L., Berton, O., Renthal, W., Russo, S. J., Laplant, Q., Graham, A., Lutter, M., Lagace, D. C., Ghose, S., Reister, R., Tannous, P., Green, T. A., Neve, R. L., Chakravarty, S., Kumar, A., Eisch, A. J., Self, D. W., … Nestler, E. J. (2007). Molecular adaptations underlying susceptibility and resistance to social defeat in brain reward regions. *Cell*, *131*(2), 391–404. https://doi.org/10.1016/j.cell.2007.09.018

Lam, K. S. L., Bodfish, J. W., & Piven, J. (2008). Evidence for three subtypes of repetitive behavior in autism that differ in familiality and association with other symptoms. *Journal of Child Psychology and Psychiatry*, *49*, 1193–1200. https://doi.org/10.1111/j.1469-7610.2008.01944.x

Lammel, S., Lim, B. K., & Malenka, R. C. (2014). Reward and aversion in a heterogeneous midbrain dopamine system. *Neuropharmacology*, *76* (Pt B(0 0)), 351–359. https://doi.org/10.1016/j.neuropharm.2013.03.019

Lefebvre, A., Traut, N., Pedoux, A., … Delorme, R. (2023). Exploring the multidimensional nature of repetitive and restricted behaviors and interests (RRBI) in autism: Neuroanatomical correlates and clinical implications. *Molecular Autism*, *14*, 45. https://doi.org/10.1186/s13229-023-00576-z

Legg, C. R., Mercier, B., & Glickstein, M. (1989). Corticopontine projection in the rat: The distribution of labelled cortical cells after large injections of horseradish peroxidase in the pontine nuclei. *Journal of Comparative Neurology*, *286*, 427–441.

Lord, C., Rutter, M., Risi, S., Gotham, K., & Bishop, S. (2012). *Autism diagnostic observation schedule* (2nd ed., p. ADOS-2). Western Psychological Corporation.

Lydon, S., Healy, O., Reed, P., Mulhern, T., Hughes, B. M., & Goodwin, M. S. (2016). A systematic review of physiological reactivity to stimuli in autism. *Developmental Neurorehabilitation*, *19*(6), 335–355. https://doi.org/10.3109/17518423.2014.971975

Mair, P., & Wilcox, R. (2019). *Robust statistical methods using WRS2*. The WRS2 Package.

Marek, S., Tervo-Clemmens, B., Calabro, F. J., Montez, D. F., Kay, B. P., Hatoum, A. S., Donohue, M. R., Foran, W., Miller, R. L., Hendrickson, T. J., Malone, S. M., Kandala, S., Feczko, E., Miranda-Dominguez, O., Graham, A. M., Earl, E. A., Perrone, A. J., Cordova, M., Doyle, O., … Dosenbach, N. U. F. (2022). Reproducible brain-wide association studies require thousands of individuals. *Nature*, *603*(7902), 654–660. https://doi.org/10.1038/s41586-022-04492-9

Martins, I., & Tavares, I. (2017). Reticular formation and pain: The past and the future. *Frontiers in Neuroanatomy*, *11*, 51. https://doi.org/10.3389/fnana.2017.00051

Mayes, S. D., & Zickgraf, H. (2019). Atypical eating behaviors in children and adolescents with autism, ADHD, other disorders, and typical development. *Research in Autism Spectrum Disorders*, *64*, 76–83.

Mire, S. S., Raff, N. S., Brewton, C. M., & Goin-Kochel, R. P. (2015). Age-related trends in treatment use for children with autism spectrum disorder. *Research in Autism Spectrum Disorders*, *15*, 29–41. https://doi.org/10.1016/j.rasd.2015.03.001

Moore, D. J. (2015). Acute pain experience in individuals with autism spectrum disorders: A review. *Autism*, *19*(4), 387–399. https://doi.org/10.1177/1362361314527839

Porges, S. W. (2003). The polyvagal theory: Phylogenetic contributions to social behavior. *Physiology & Behavior*, *79*(3), 503–513.

Porges, S. W. (2005). The vagus: A mediator of behavioral and physiologic features associated with autism. *The Neurobiology of Autism*, *2*, 65–77.

R Core Team. (2023). *R: A language and environment for statistical computing*. R Foundation for Statistical Computing https://www.R-project.org/

Ramos, J. M., & Puerto, A. (1988). The nucleus parvocellularis reticularis regulates submandibular-sublingual salivary secretion in the rat: A pharmacological study. *Journal of the Autonomic Nervous System*, *23*(3), 221–228.

Revelle, W. (2023). Psych: Procedures for psychological, psychometric, and personality research. Northwestern University. https://CRAN.R-project.org/package=psych

Rimland, B. (1964). Infantile autism: The syndrome and its implications for a neural theory of behavior. Appleton-Century-Crofts. https://books.google.es/books?id=dtFsAAAAMAAJ

Rutter, M., Bailey, A., & Lord, C. (2003). *The social communication questionnaire*. Western Psychological Services.

Rutter, M., Le Couteur, A., & Lord, C. (2003). *Autism diagnostic interview-revised*. Western Psychological Services.

Schuetze, M., Park, M., Cho, I., MacMaster, F. P., Chakravarty, M. M., & Bray, S. L. (2016). Morphological alterations in the thalamus, striatum, and pallidum in autism spectrum disorder. *Neuropsychopharmacology*, *41*, 2627–2637. https://doi.org/10.1038/npp.2016.64

Shammah-Lagnado, S. J., Costa, M., & Ricardo, J. A. (1992). Afferent connections of the parvocellular reticular formation: A horseradish peroxidase study in the rat. *Neuroscience*, *50*(2), 403–425.

Singh, K., García-Gomar, M. G., & Bianciardi, M. (2021). Probabilistic atlas of the mesencephalic reticular formation, isthmic reticular formation, microcellular tegmental nucleus, ventral tegmental area nucleus complex, and caudal-rostral linear raphe nucleus complex in living humans from 7 Tesla magnetic resonance imaging. *Brain Connectivity*, *11*(8), 613–623. https://doi.org/10.1089/brain.2020.0975

Singh, K., García-Gomar, M. G., Cauzzo, S., Staab, J. P., Indovina, I., & Bianciardi, M. (2022). Structural connectivity of autonomic, pain, limbic, and sensory brainstem nuclei in living

humans based on 7 Tesla and 3 Tesla MRI. *Human Brain Mapping*, *43*(10), 3086–3112. https://doi.org/10.1002/hbm.25836

Singh, K., Indovina, I., Augustinack, J. C., Nestor, K., García-Gomar, M. G., Staab, J. P., & Bianciardi, M. (2019). Probabilistic template of the lateral parabrachial nucleus, medial parabrachial nucleus, vestibular nuclei complex, and medullary viscero-sensory-motor nuclei complex in living humans from 7 Tesla MRI. *Frontiers in Neuroscience*, *13*, 1425. https://doi.org/10.3389/fnins.2019.01425

Sitek, K. R., Gulban, O. F., Calabrese, E., Johnson, G. A., Lage-Castellanos, A., Moerel, M., Ghosh, S. S., & De Martino, F. (2019). Mapping the human subcortical auditory system using histology, postmortem MRI and in vivo MRI at 7T. *eLife*, *8*, e48932. https://doi.org/10.7554/eLife.48932

Stüber, C., Morawski, M., Schäfer, A., Labadie, C., Wähnert, M., Leuze, C., Streicher, M., Barapatre, N., Reimann, K., Geyer, S., Spemann, D., & Turner, R. (2014). Myelin and iron concentration in the human brain: A quantitative study of MRI contrast. *NeuroImage*, *93*(Pt 1), 95–106. https://doi.org/10.1016/j.neuroimage.2014.02.026

Sun, L., Liu, R., Guo, F., Wen, M.-Q., Ma, X.-L., Li, K.-Y., Sun, H., Xu, C.-L., Li, Y.-Y., Wu, M.-Y., Zhu, Z.-G., Li, X.-J., Yu, Y.-Q., Chen, Z., Li, X.-Y., & Duan, S. (2020). Parabrachial nucleus circuit governs neuropathic pain-like behavior. *Nature Communications*, *11*(1), 5974. https://doi.org/10.1038/s41467-020-19767-w

Supekar, K., Ryali, S., Mistry, P., & Menon, V. (2021). Aberrant dynamics of cognitive control and motor circuits predict distinct restricted and repetitive behaviors in children with autism. *Nature Communications*, *12*, 3537. https://doi.org/10.1038/s41467-021-23822-5

Surgent, O., Guerrero-Gonzalez, J., Dean, D. C., 3rd, Kirk, G. R., Adluru, N., Kecskemeti, S. R., Alexander, A. L., & Travers, B. G. (2023). How we get a grip: Microstructural neural correlates of manual grip strength in children. *NeuroImage*, *273*, 120117. https://doi.org/10.1016/j.neuroimage.2023.120117

Surgent, O., Riaz, A., Ausderau, K. K., Adluru, N., Kirk, G. R., Guerrero-Gonzalez, J., Skaletski, E. C., Kecskemeti, S. R., Dean Iii, D. C., Weismer, S. E., Alexander, A. L., & Travers, B. G. (2022). Brainstem white matter microstructure is associated with hyporesponsiveness and overall sensory features in autistic children. *Molecular Autism*, *13*(1), 48. https://doi.org/10.1186/s13229-022-00524-3

Ter Horst, G., Copray, J., Liem, R., & Van Willigen, J. (1991). Projections from the rostral parvocellular reticular formation to pontine and medullary nuclei in the rat: Involvement in autonomic regulation and orofacial motor control. *Neuroscience*, *40*(3), 735–758.

Tervo, D. G. R., Hwang, B. Y., Viswanathan, S., Gaj, T., Lavzin, M., Ritola, K. D., … Karpova, A. Y. (2016). A designer AAV variant permits efficient retrograde access to projection neurons. *Neuron*, *92*(2), 372–382. https://doi.org/10.1016/j.neuron.2016.09.021

Thayer, J. F., & Lane, R. D. (2000). A model of neurovisceral integration in emotion regulation and dysregulation. *Journal of Affective Disorders*, *61*(3), 201–216. https://doi.org/10.1016/s0165-0327(00)00338-4

Travers, B. G., Bigler, E. D., Tromp, D. P. M., Adluru, N., Destiche, D., Samsin, D., Froehlich, A., Prigge, M. D. B., Duffield, T. C., Lange, N., Alexander, A. L., & Lainhart, J. E. (2015). Brainstem white matter predicts individual differences in manual motor difficulties and symptom severity in autism. *Journal of Autism and Developmental Disorders*, *45*(9), 3030–3040. https://doi.org/10.1007/s10803-015-2467-9

Travers, J. B., Dinardo, L. A., & Karimnamazi, H. (1997). Motor and premotor mechanisms of licking. *Neuroscience & Biobehavioral Reviews*, *21*(5), 631–647.

Trevarthen, C., & Delafield-Butt, J. T. (2013). Autism as a developmental disorder in intentional movement and affective engagement. *Frontiers in Integrative Neuroscience*, *7*, 49. https://doi.org/10.3389/fnint.2013.00049

Venkatraman, A., Edlow, B. L., & Immordino-Yang, M. H. (2017). The brainstem in emotion: A review. *Frontiers in Neuroanatomy*, *11*, 15. https://doi.org/10.3389/fnana.2017.00015

Veraart, J., Novikov, D. S., Christiaens, D., Ades-Aron, B., Sijbers, J., & Fieremans, E. (2016). Denoising of diffusion MRI using random matrix theory. *NeuroImage*, *142*, 394–406. https://doi.org/10.1016/j.neuroimage.2016.08.016

Weeland, C. J., Kasprzak, S., de Joode, N. T., Abe, Y., Alonso, P., Ameis, S. H., Anticevic, A., Arnold, P. D., Balachander, S., Banaj, N., Bargallo, N., Batistuzzo, M. C., Benedetti, F., Beucke, J. C., Bollettini, I., Brecke, V., Brem, S., Cappi, C., Cheng, Y., … Vriend, C. (2022). The thalamus and its subnuclei—A gateway to obsessive-compulsive disorder. *Translational Psychiatry*, *12*, 70. https://doi.org/10.1038/s41398-022-01823-2

Xavier, J., Bursztejn, C., Stiskin, M., Canitano, R., & Cohen, D. (2015). Autism spectrum disorders: An historical synthesis and a multidimensional assessment toward a tailored therapeutic program. *Research in Autism Spectrum Disorders*, *18*, 21–33. https://doi.org/10.1016/j.rasd.2015.06.011

Yadid, G., & Friedman, A. (2008). Dynamics of the dopaminergic system as a key component to the understanding of depression. *Progress in Brain Research*, *172*, 265–286. https://doi.org/10.1016/S0079-6123(08)00913-8

Zhang, H., Schneider, T., Wheeler-Kingshott, C. A., & Alexander, D. C. (2012). NODDI: Practical in vivo neurite orientation dispersion and density imaging of the human brain. *NeuroImage*, *61*(4), 1000–1016. https://doi.org/10.1016/j.neuroimage.2012.03.072

SUPPORTING INFORMATION

Additional supporting information can be found online in the Supporting Information section at the end of this article.